

Dynamic structure factor $S(q,\omega)$ of metallic lithium by X-ray inelastic scattering

This article has been downloaded from IOPscience. Please scroll down to see the full text article.

1989 J. Phys.: Condens. Matter 1 5187

(<http://iopscience.iop.org/0953-8984/1/31/018>)

View [the table of contents for this issue](#), or go to the [journal homepage](#) for more

Download details:

IP Address: 171.66.16.93

The article was downloaded on 10/05/2010 at 18:33

Please note that [terms and conditions apply](#).

Dynamic structure factor $S(q, \omega)$ of metallic lithium by x-ray inelastic scattering

T Suzuki[†], A Tanokura[†] and N Arimitsu[‡]

[†] Department of Physics, Sophia University, Chiyoda-ku, Kioi-cho, Tokyo 102

[‡] Division of Electrical and Computer Engineering, Faculty of Engineering, Yokohama National University, Hodogaya-ku, Tokiwadai, Yokohama 240

Received 6 January 1989

Abstract. Characteristics of x-ray inelastic scattering by metallic lithium were observed over a wide range of transferred momentum, q , using incident x-rays of CuK β . The spectral profile consisted of two contributions, from core electrons and valence electrons, which overlap totally in larger q and become separate from each other at smaller q . The spectra also depend on energy transfer, ω . The corresponding dynamic structure factor $S(q, \omega)$ was theoretically computed. For valence electrons, the impulse approximation was first applied for all values of q , and then random phase approximation was applied for smaller q . For core electrons, the one-site approximation was applied. Agreement between the experimental result and the theoretical computation is fairly good.

1. Introduction

A revival of investigations on x-ray Compton scattering was initiated by the study concerning electronic states of valence electrons in metallic lithium (March 1954, Cooper *et al* 1965, Stuewer and Cooper 1977). During the investigation, so called x-ray Raman scattering was found (Das Gupta 1959, Suzuki 1966, Mizuno and Ohmura 1967, Suzuki 1967, Suzuki *et al* 1970, Kuriyama 1971, Suzuki and Nagasawa 1975, Kuriyama and Alexandropoulos 1971); this came from core electrons. Furthermore, x-ray plasmon scattering by valence electrons, which was suggested by Nozières and Pines (1959) and Ohmura and Matsudaira (1964), was detected experimentally (Priftis *et al* 1968, Tanokura *et al* 1969, Suzuki and Tanokura 1970, 1971, Priftis *et al* 1978). Thus the research region of x-ray inelastic scattering, hitherto called Compton scattering, has been expanded to cover wider ranges of transferred momentum and to concern not only valence electrons but also core electrons as a whole (Bushuev and Kuz'min 1977, Suzuki 1982). A study may be made to obtain information on elementary scattering process between x-ray photons and electrons and fundamental electronic states in solids. Such a work is referred to, in general, as a study on the dynamic structure factor $S(q, \omega)$ of solids by x-ray inelastic scattering, e.g. Vradsis and Priftis (1985) or Arimitsu *et al* (1987). Here, q and ω are the momentum and energy transferred from incident x-ray photons to electrons in solids, respectively, in Slater's atomic units[†], e.g. Callaway (1964).

[†] For the expression and computation in this paper, Slater's atomic units (abridged as au) are employed, where action, length and energy are measured in units of \hbar , the Bohr radius and the Rydberg energy, respectively.

Although there have been several studies on Compton scattering by lithium, as listed in the paper of Suzuki and Nagasawa (1981), most of them have dealt with transferred momenta of high q . In this study, $S(\mathbf{q}, \omega)$ of polycrystalline metallic lithium was observed over a wide range of q between 0.63 and 3.38 au using incident x-rays of Cu $K\beta$, where contributions from core electrons should play an important role. The present experiment was planned to develop the previous work of Suzuki and Nagasawa (1981). The spectral profiles observed were analysed theoretically. For valence electrons, the analysis was at first based upon the impulse approximation for all values of q , then took into account the random phase approximation (RPA) for smaller q . For core electrons the one-site approximation was applied. This approximation is situated between the impulse- and the dipole-approximation; its detailed description is in the theoretical § 3. The experimental results and the theoretical evaluation are compared and discussed in § 4, with reference being made to previous works.

2. Experiment

The incident x-rays were Cu $K\beta$ of $\lambda = 1.39 \text{ \AA}$ and $E = 8.9 \text{ keV}$. A sealed-off x-ray tube was operated at 40 keV and 20 mA with a stability of $\pm 0.1\%$ by a feedback system in the secondary output circuits. Blocks of metallic lithium with a purity of 99.9% were obtained from Koch-Light Lab. The effect of multiple scattering was preliminarily examined by observing spectral profiles at a fixed scattering angle of 90° with several samples of different thicknesses from 0.35 to 15.0 mm. Little difference in spectral profiles for different samples was found. The mean free path is 30 mm, the evaluation being based upon the mass absorption coefficient of the relevant x-rays in metallic lithium. Therefore square specimens with 3 mm thickness and 10 mm sides were cut from the block matrix. The path lengths of the x-rays in the specimen suggest that this thickness was small enough to eliminate the effect of multiple scattering. A two-crystal energy analyser was employed in which the LiF single crystal (200) reflections in (+, +) position were detected. Treatments of samples, instrumentation and procedures in intensity measurement were the same as those in the previous report of Suzuki and Nagasawa (1981).

The intensity measurements were performed at scattering angles of $\theta = 15, 25, 45$ and 90° . The angle θ is between the incident x-rays and the scattered x-rays, whose energy was analysed with the two-crystal energy analyser. The scattering angles above cover the range of transferred momentum, q , between 0.63 and 3.38 au. Here it should be mentioned that q is not simply proportional to $\sin(\theta/2)$, but also depends on energy loss ω .

Subtraction of the component of elastic and thermal diffuse scattering was carried out applying the dummy experimental method, similar to that reported by Priftis (1970). In the process of the subtraction, the criterion was that no minus value nor any apparent irregularities in the resultant spectral profiles should appear. An absorption correction for intensity was applied for each scattering angle according to the different path length of the x-rays in every case.

3. Theory

The differential scattering cross section can be expressed as

$$(d^2\sigma/d\Omega d\omega) = r_0^2[(1 + \cos^2\theta)/2](\omega/\omega_0)NS(\mathbf{q}, \omega) \quad (1)$$

where $r_0 (= e^2/mc^2)$ is the classical radius of the electron, θ is the scattering angle, ω_0

and ω_1 are the energies of incident and scattered x-rays, respectively, N is the number of unit cells in the crystal, and $\mathbf{q} (= \mathbf{k}_0 - \mathbf{k}_1)$ and $\omega (= \omega_0 - \omega_1)$ are transferred momentum and energy from incident x-ray photons to electrons in solids, respectively, denoted in atomic unit ($\hbar = 1$). The wavevectors of the incident and scattered x-rays are expressed by \mathbf{k}_0 and \mathbf{k}_1 , respectively. The transferred momentum q is a function of not only the scattering angle θ but also of the energy ω_0 and ω as follows

$$q = [\omega^2 + 2\omega_0(\omega_0 - \omega)(1 - \cos \theta)]^{1/2}/c \tag{2a}$$

$$q_0 \equiv q(\omega = 0) = 2\omega_0 \sin(\theta/2)/c \tag{2b}$$

$S(\mathbf{q}, \omega)$ is the dynamic structure factor per unit cell. If the one-electron approximation is adopted, $S(\mathbf{q}, \omega)$ may be written as

$$S(\mathbf{q}, \omega) = 2N^{-1} \sum_i \sum_f n_i(1 - n_f) |\langle \psi_f | e^{i\mathbf{q}\cdot\mathbf{r}} | \psi_i \rangle|^2 \delta(\omega - \varepsilon_f + \varepsilon_i) \tag{3}$$

where ψ_i and ψ_f represent one-electron orbitals for initial and final states, respectively, ε_i and ε_f being the energy of these orbitals. The factor of 2 comes from the fact that every orbital state is occupied by two electrons. n_i and n_f represent occupation numbers in state i and state f , respectively. As $\sum_i n_i$ denotes the summation over all occupied orbitals, $S(\mathbf{q}, \omega)$ can be decomposed into two parts

$$S(\mathbf{q}, \omega) = S_v(\mathbf{q}, \omega) + S_c(\mathbf{q}, \omega). \tag{4}$$

Here S_v and S_c correspond to valence and core electrons in orbital state i , respectively. This decomposition is valid if correlations between valence and core electrons are not taken into account.

In many theoretical treatments of x-ray inelastic scattering the impulse approximation is applied to both kinds of electrons. In general, however, this approximation is considered as becoming poorer with decreasing q for core electrons much more rapidly than for valence electrons.

3.1. The $S_v(\mathbf{q}, \omega)$

First we consider the $S_v(\mathbf{q}, \omega)$. As regards the valence electrons, the impulse approximation will be safely applied except when $q < 2k_F$, k_F being the Fermi momentum of the valence electron. In the impulse approximation (Chew and Wick 1952, Cooper 1971) the scattering electron has been considered to be a free electron. If the interaction time is sufficiently short, the position of this electron remains essentially constant for the duration of the interaction. Then the potential energy term immediately after collision is the same as it was immediately before the collision.

Many theoretical studies have been done for $S_v(\mathbf{q}, \omega)$ within the impulse approximation. In the present paper we adopted the numerical data given by Phillips and Weiss (1972), in which the correlations between valence electrons were taken into account. Over three crystallographic directions they averaged the results obtained for a single crystal by using the approach of Lundqvist and Lydén (1971). In this approach, $S_v(\mathbf{q}, \omega)$ was written as

$$S_v(\mathbf{q}, \omega) = 2N^{-1} \sum_i n_i \int \int_{p_z=|z|} |\chi_i(p_x, p_y, p_z)|^2 \frac{1}{2q} dp_x dp_y \tag{5}$$

where

$$z = \omega/2q - q/2. \tag{6}$$

Here z axis is chosen parallel to the direction of the scattering vector \mathbf{q} . The modification

from (3) to (5) is given by Mendelsohn and Smith (1977). χ_i is the Fourier transform of the wavefunction ψ_i in (3). In the one-electron approximation 0 or 1 is substituted into n_i , but they used electron-gas data which Lundqvist (1968) obtained, namely an intermediate value between 0 and 1. They calculated χ_i using the orthogonal plane wave (OPW) method with 19 plane waves with parameters from Callaway (1958, 1961, 1963). In case of $q < 2k_F$, the impulse approximation is inadequate. Hence we used another approximation, studied by Ohmura and Matsudaira (1964), in which the Pauli principle based upon the Hartree–Fock approximation and the Coulomb shielding effect of valence electrons within the RPA are taken into account.

3.2. The $S_c(\mathbf{q}, \omega)$

Next we consider the $S_c(\mathbf{q}, \omega)$. The product of the mean orbital radius, a , of the core electron and q is denoted by $\alpha (=aq)$. The criteria of the validity of approximation can be classified as follows.

(i) $\alpha \gg 1$. The impulse approximation can be applied and the scattering is Compton-like. Within the one-electron approximation ($n_i = 1$), $S_c(\mathbf{q}, \omega)$ may be written as

$$S_c(\mathbf{q}, \omega) = 2 \sum_k |\langle \psi_k | e^{i\mathbf{q}\cdot\mathbf{r}} | \psi_c \rangle|^2 \delta(\omega - 2\mathbf{k} \cdot \mathbf{q} + q^2) \quad (7)$$

where ψ_k denotes the free-electron wave function with wavenumber k , and ψ_c represents the 1s atomic orbital. However, the energy is regarded as free-electron type.

(ii) $\alpha \ll 1$. The dipole approximation is applicable and the scattering is Raman-type. Within the one-electron approximation $S_c(\mathbf{q}, \omega)$ can be written as

$$S_c(\mathbf{q}, \omega) = 2 \sum_f (1 - n_f) |\langle \psi_f | i\mathbf{q} \cdot \mathbf{r} | \psi_c \rangle|^2 \delta(\omega - \varepsilon_f + \varepsilon_c) \quad (8)$$

where ψ_f is an unoccupied orbital and ε_f denotes its energy. The energy of the 1s atomic orbital is denoted by ε_c .

(iii) $\alpha \approx 1$. Neither of the above approximations are valid. In the present experiment the value α lies between 0.2–1.2, because the ‘ a ’ of core electrons in lithium is 0.37 au. Arimitsu *et al* (1987) have performed a theoretical study of $S_c(\mathbf{q}, \omega)$ of metallic lithium to analyse the results of the present experiment. They adopted an additional approximation, besides the one-electron approximation. They replaced the periodic potential by one that was constant except within a sphere with its centre at the nucleus of the ion in question. As a result, the situation could be reduced to one-centre problem and ψ_f may be written as the spherical wave function. $S_c(\mathbf{q}, \omega)$ may be written as

$$S_c(\mathbf{q}, \omega) = 2 \sum_k \sum_l \sum_m |\langle \psi_{klm} | e^{i\mathbf{q}\cdot\mathbf{r}} | \psi_c \rangle|^2 \delta(\omega - \varepsilon_{kl} + \varepsilon_c) \quad (9)$$

where

$$\varepsilon_{kl} = \gamma_s(r_0) + k^2 \quad (k \geq 0). \quad (10)$$

Here l and m denote the orbital angular momentum and the magnetic quantum number, respectively, and $\gamma_s(r_0)$ represents a constant value outside the sphere of a radius r_0 . They called this method as ‘the one-site approximation’. Details of the approach are given in their paper.

4. Results and discussion

In figure 1 computed profiles of $S(\mathbf{q}, \omega)$ corresponding to the experimental scattering angles $\theta = 90, 45, 25$ and 15° are shown; these denote separately, for each θ , the contribution of valence electrons (proportional to S_v) and that of the core electrons (proportional to S_c). At scattering angles $\theta = 90^\circ$ and 45° the contributions overlap each other, and their summed resultant profiles ($S_v + S_c$) are shown in parts (a) and (b) by bold curves. At $\theta = 25^\circ$ and 15° , S_v and S_c are completely separated from each other, as is shown in parts (c) and (d), because the cut-off edge of S_c remains fixed at 55 eV and the peak position of S_v moves with the well known Compton shift. With decreasing scattering angle, the cross section for S_c becomes very small, while that for S_v becomes larger at its peak value and narrower.

For the valence electrons, only the results of impulse approximation are shown in figure 1. In general, for smaller scattering angle θ , that is for smaller q , the RPA should

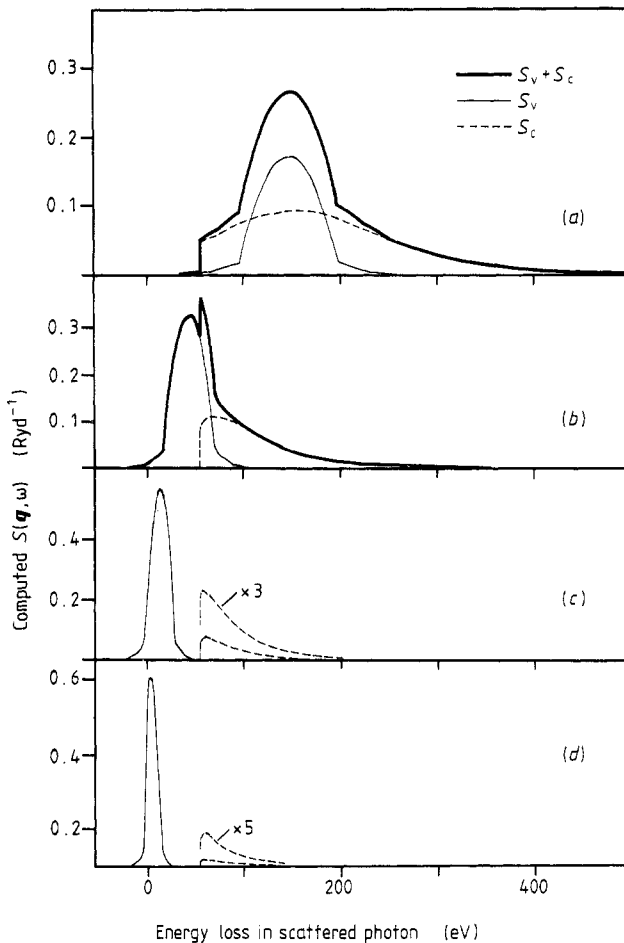


Figure 1. Computed profiles for $S(\mathbf{q}, \omega)$. The values for θ , the scattering angle, and q_0 , as defined in equation (2b), are for (a), $\theta = 90^\circ$, $q_0 = 3.38$ au; (b), $\theta = 45^\circ$, $q_0 = 1.83$ au; (c) $\theta = 25^\circ$, $q_0 = 1.03$ au; and (d), $\theta = 15^\circ$, $q_0 = 0.63$ au. Thin full curves, broken curves and bold curves correspond to $S_v(\mathbf{q}, \omega)$, $S_c(\mathbf{q}, \omega)$ and total $S(\mathbf{q}, \omega)$, respectively.

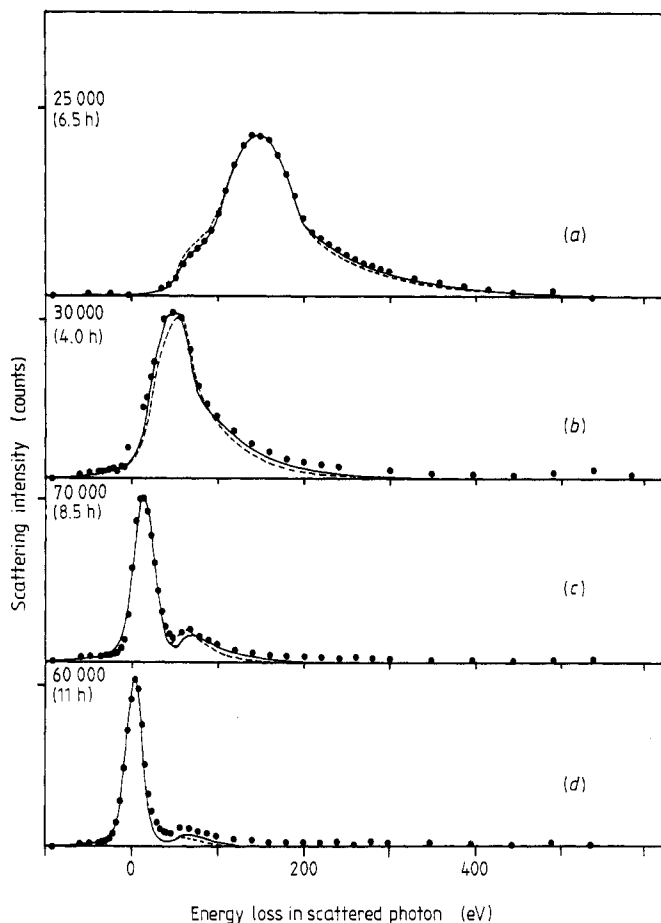


Figure 2. Comparison between the computed and observed (full circles) profiles of $S(\mathbf{q}, \omega)$, where the computed profiles were convoluted by a resolution function shown in an inset in figure 3. Their highest peak values are normalised to the same height in each figure. The values for θ , the scattering angle, and q_0 , as defined in equation (2b), are for (a), $\theta = 90^\circ$, $q_0 = 3.38$ au; (b) $\theta = 45^\circ$, $q_0 = 1.83$ au; (c), $\theta = 25^\circ$, $q_0 = 1.03$ au; and (d), $\theta = 15^\circ$, $q_0 = 0.63$ au. Full curves, impulse approximation for S_v ; one-site approximation for S_c ; broken curves, impulse approximation for S_v and S_c .

be taken into account. In the present study the scattering angle $\theta = 15^\circ$ corresponds to such a case; it will be discussed later.

In figure 2, the experimental results are shown (with filled circles) and compared with the theoretically evaluated spectral profiles ($S_v + S_c$) mentioned above. For comparison, the theoretical profiles (drawn with fine solid curves) were convoluted with a resolution function. The resolution function has a half-width of 15 eV, as shown in the inset in figure 3; it includes both the natural linewidths of the incident radiation and the instrumental broadening. Therefore, fine structures in the computed profile, such as shown in figure 1(b), were smeared out. The theoretical and experimental results were normalised at the maximum peak height of each profile.

In figure 2, trial computed results are also shown (with broken curves). They were obtained with the impulse approximation for both core and valence electrons, except

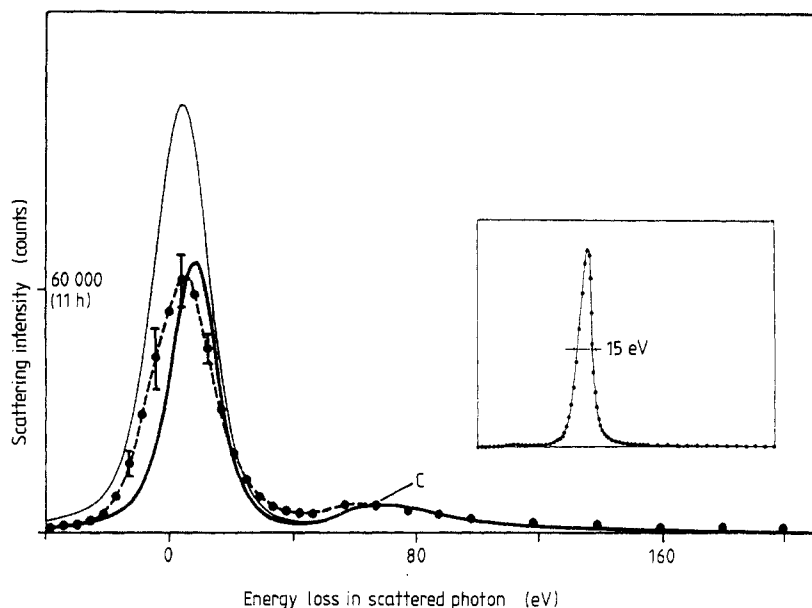


Figure 3. Comparison between the computed and observed profile of $S(\mathbf{q}, \omega)$ at $\theta = 15^\circ$ and $q_0 = 0.63$ au. Observed profile is denoted by a broken curve with solid circles. The thin full curve corresponds to the curves in figure 2(d). The bold full curve is a result computed with the RPA. Both theoretical curves were convoluted by the experimental resolution function shown in the inset. The contribution from core electrons is normalised to the same height for each curve, labelled C.

that the cut-off at the binding energy of 55 eV for core electrons was taken into account. The broken curves almost coincide with the solid curves. However, taken as a whole, the solid curves, based upon a higher approximation, fit better with the experimental results than the broken curves, based on a lower approximation.

In figure 3, results of computation with and without the RPA are shown. For q smaller than $2k_F$, it is to be expected that the impulse approximation would not be adequate even for valence electrons. Such a situation occurs at $\theta = 15^\circ$ under the present experimental conditions. The situation can be improved by using the RPA for valence electrons. The thick solid curve was computed with the RPA and the thin solid curve only with the impulse approximation. The broken curve with solid circles is the experimental profile. All these three profiles are normalised with respect to the contribution from the core electrons, because accuracy for both the theoretical and also the experimental treatment is better in this region. Agreement between the theoretical profiles and the experimental one is not satisfactory. However, agreement is far better with the RPA than without it, at least with respect to the peak height of the valence electron contribution. It should be mentioned here that in figure 2 theoretical and experimental profiles are normalised to the same height in each scattering angle. In figure 2(d), therefore, the theoretical profile of core electron contribution was much smaller than the experimental one. The method of comparison given in figure 3 is more meaningful than that in figure 2(d).

This study on the dynamic structure factor $S(\mathbf{q}, \omega)$ of metallic lithium by x-ray scattering under the present conditions can be connected with the results of previous study (Suzuki and Nagasawa 1981), where the scattering angle θ was 140° . Putting together the results of both studies, we can conclude as follows.

In general, for larger q , both core and valence electrons cause the well known Compton scattering. However, for smaller q and light element solids, they behave in quite different ways.

(i) At larger q . (a) Valence electrons react in almost same way as in the typical Compton scattering. However, the shift of the profile peak is not simply Compton-like, because the momentum transfer q is not constant at fixed θ , but should be expressed by equation (2a). Theoretically, the impulse approximation can be applied. The profile of S_v is nearly parabolic, accompanied with small tails caused by the many-body effect. (b) Although core electrons also react in a Compton-like way, the profile of S_c is not parabolic, but has a long tail to the right side and a cut-off edge to the left side. The former is caused by initial states of the electrons and the latter is due to the binding energy of the electrons.

(ii) At smaller q , in other words $\alpha \ll 1$. Core electrons cause x-ray Raman scattering, with the maximum cross section near the fixed cut-off edge. To compute S_c , neither the impulse nor the dipole approximation is applicable; the one-site approximation described in § 3 is most suitable.

(iii) Contributions from both kinds of electrons overlap each other at larger q ($q_0 = 3.38$ and 1.83 au in the present case) and become separate from each other at smaller q ($q_0 = 1.03$ and 0.63 au in the present case).

(iv) For much smaller q ($q_0 = 0.63$ au in the present case). Valence electrons cause the plasmon scattering. In such a case, the impulse approximation was inadequate even for valence electrons. The random phase approximation (RPA) was effective, but discrepancies with the experimental results still remain, as already pointed out by Priftis *et al* (1978).

(v) Experiments with much better resolution could reveal interesting fine structures. Using a sealed-off x-ray tube, however, it is impossible to get much better resolution than in the present study, because of the very small scattering cross section. A strong x-ray source of synchrotron radiation (SOR) should provide much more interesting information concerning the electronic state in light element solids, e.g. Schülke *et al* (1984), Schülke *et al* (1986) and Nagasawa (1987). Such work should stimulate the theoretical treatments regarding their dynamical structure factor $S(\mathbf{q}, \omega)$.

Acknowledgments

We would like to thank professor Y Ohmura and Dr H Nagasawa for their incessant interest to this work. We gratefully acknowledge Professor Y Mizuno for his valuable discussion and instruction, especially regarding the theoretical part.

References

- Arimitsu N, Kobayashi Y and Mizuno Y 1987 *J. Phys. Soc. Japan* **56** 2940
- Bushuev V A and Kuz'min R N 1977 *Sov. Phys.-Usp.* **20** 406
- Callaway J 1958 *Phys. Rev.* **109** 1541
- 1961 *Phys. Rev.* **124** 1824
- 1963 *Phys. Rev.* **131** 2839
- 1964 *Energy Band Theory* (New York: Academic) p 55
- Chew G F and Wick G C 1952 *Phys. Rev.* **85** 636

- Cooper M 1971 *Adv. Phys.* **20** 453
Cooper M, Leake J A and Weiss R J 1965 *Phil. Mag.* **12** 797
Das Gupta K 1959 *Phys. Rev. Lett.* **3** 38
Kuriyama M 1971 *Acta Crystallogr. A* **27** 634
Kuriyama M and Alexandropoulos N G 1971 *Phys. Soc. Japan* **31** 561
Lundqvist B I 1968 *Phys. Kond. Mater.* **7** 117
Lundqvist B I and Lydén C 1971 *Phys. Rev. B* **4** 3360
March N H 1954 *Proc. Phys. Soc. A* **67** 9
Mendelsohn L and Smith V H 1977 *Compton Scattering* ed. B G Williams (New York: McGraw-Hill) p 102
Mizuno Y and Ohmura Y 1967 *J. Phys. Soc. Japan* **22** 445
Nagasawa H 1987 *J. Physique* **48** C9-863
Nozières P and Pines D 1959 *Phys. Rev.* **113** 1254
Ohmura Y and Matsudaira N 1964 *J. Phys. Soc. Japan* **19** 1355
Phillips W C and Weiss R J 1972 *Phys. Rev. B* **5** 755
Priftis G D 1970 *Phys. Rev. B* **2** 54
Priftis G D, Boviatsis J and Vradis A 1978 *Phys. Lett.* **68A** 482
Priftis G D, Theodossiou A and Alexopoulos K D 1968 *Phys. Lett.* **27A** 577
Schülke W, Nagasawa H and Mourikis S 1984 *Phys. Rev. Lett.* **52** 2065
Schülke W, Nagasawa H, Mourikis S and Lanzki P 1986 *Phys. Rev. B* **33** 6744
Stuewer R H and Cooper M J 1977 *Compton Scattering* ed. B G Williams (New York: McGraw-Hill) ch 1
Suzuki T 1966 *J. Phys. Soc. Japan* **21** 2087
— 1967 *J. Phys. Soc. Japan* **22** 1139
— 1982 *Advances in X-Ray Spectroscopy* ed. C Bonnelle and C Mandé (Oxford: Pergamon) ch 23
Suzuki T and Tanokura A 1970 *J. Phys. Soc. Japan* **28** 1382
Suzuki T, Kishimoto T, Kaji T and Suzuki T 1970 *J. Phys. Soc. Japan* **29** 730
Suzuki T and Nagasawa H 1975 *J. Phys. Soc. Japan* **39** 1597
— 1981 *J. Phys. C: Solid State Phys.* **14** 1783
Tanokura A, Hirota N and Suzuki T 1969 *J. Phys. Soc. Japan* **27** 151
Vradis A and Priftis G D 1985 *Phys. Rev. B* **32** 3556